# Vulnerability of rare-earth-doped fibers for space missions: origins of radiation-induced attenuation

Y. Ouerdane[*a], S. Girard[b], B. Tortech[a], T. Robin[c], C. Marcandella[b], A. Boukenter[a], B. Cadier[c], J.-P. Meunier[a], P. Crochet[c]

[a] LAboratoire Hubert Curien (LAHC), UMR-CNRS 5516, F42000 Saint-Etienne, France
[b]CEA, DAM, DIF, F91297 Arpajon, France
[c] iXFiber SAS, F22300 Lannion, France

## ABSTRACT

We characterized the responses of different types of rare-earth doped fibers (Yb, Er and Er/Yb) to various types of radiations like UV, gamma-rays, X-rays and protons. The understanding of the radiation-induced effects in this class of optical fibers is necessary as they are possible candidates for use as part of fiber-based systems like gyroscopes that will have to operate in space environment. For all types of irradiations, the main effect is an increase of the linear absorption of these waveguides due to the generation of point defects in the core and cladding. We characterize the growth and decay kinetics of the radiation-induced attenuation during and after irradiation for various compositions of optical fibers. In this paper, we particularly investigate the relative influence of the rare-earth ions (Er, Yb or Er/Yb) and of the glass matrix dopants (Al, P, ...) on the optical degradation induced by ultraviolet laser exposure at 5 eV. This has been done by using a set of five prototype optical fibers designed by iXFiber SAS to enlighten the role of these parameters. Additional spectroscopic tools like confocal microscopy of luminescence are also used to detect possible changes in the spectroscopy of the rare-earth ions and their consequence on the functionality of the active optical fibers.

**Keywords:** radiations, optical fibers, attenuation, rare-earths, Erbium, Ytterbium

## 1. INTRODUCTION

Radiations generate point defects in dielectrics like amorphous silica (a-$SiO_2$) through ionization or knock-on processes [1-3]. These point defects are responsible for the degradation of the macroscopic properties of silica-based devices in harsh environments [4]. It has been shown that the amplitude and the kinetics of these changes are related to the stability and to the optical or electrical properties of these radiation-induced point defects. As an example, radiations generate leakage current increase for microelectronic components or degrade the transmission capability of optical fibers. In this paper, we investigated the generation mechanisms and the spectroscopic properties of the point defects responsible for the radiation sensitivity of silica-based optical fibers. For these devices, previous studies pointed out three possible degradation mechanisms: radiation-induced attenuation (RIA), radiation-induced luminescence (RIL) and radiation-induced compaction [5-9]. For most of the applications, the RIA will be the limiting effect, its amplitude and kinetics during and after irradiation depend on the nature of the generated point defects. RIL can be the limiting parameters for high dose rate exposures or for waveguides exhibiting low induced losses. Compaction seems to mainly occur for environments characterized by very high dose levels. The space environment [10] is characterized by low dose rate and the total dose associated with a space mission remains limited to quite low doses (<100 krad) explaining why the RIA measurement is the key factor to estimate the vulnerability of an optical fiber to these radiative conditions.

A lot of intrinsic and extrinsic parameters like the glass composition, the fabrication process parameters, temperature will affect its radiation sensitivity [11-14]. Among the different classes of optical fibers, Rare-Earth (RE)-doped optical

[*] ouerdane@univ-st-etienne.fr; phone +33 4 77 91 58 13

Fiber Optic Sensors and Applications VI, edited by Eric Udd, Henry H. Du, Anbo Wang, Proc. of SPIE Vol. 7316, 731617

fibers have been shown to be very sensitive to ionizing radiations (like γ-rays, protons,…) compared to other passive (RE-free) fibers. This higher sensitivity explains that the vulnerability of this type of optical fibers has to be characterized despite the small length typically used for most of their possible applications in radiative environment.

We recently proposed different experiments [15-16] to offer a better understanding of the radiation-induced effects in RE- doped optical fibers. Concerning Er-doped optical fibers, our results showed that two different classes can be considered: Al-doped and Al-free Er-doped samples. For the first ones, it seems that the concentration of the rare-earth ions can change the glass radiation sensitivity whereas for Al-doped silica-based fibers, it seems that this parameter does not affect the radiation response. On the contrary, based on our results and those of previous studies, it seems that an increase of the Al dopant concentration increases the loss levels with a saturation point for concentrations larger than few percent (~5%). We showed by comparing the radiation-induced absorption spectra of Al-doped SMF and Al-doped Er-doped fibers in the infrared range (900-1700nm) that the point defects present in the Er-free samples are able to reproduce the spectral dependence of RIA in the Er-doped fibers. That means that there are no point defects specific to the rare-earth ions. Most of them are probably related to the host matrix: silica-based glass with dopants like germanium (Ge), fluorine (F), phosphorus (P) or Aluminum (Al).

We also recently studied the vulnerability of Ytterbium-doped optical fibers as they are promising for space applications. In [spieOFS08], we used the confocal microscopy of luminescence tool to study the spectroscopic properties of point defects in the visible range for a set of five different samples (3 Yb-doped fibers and 2 Yb/Er-doped samples). These post-mortem analyses revealed some of the differences in radiation-induced changes depending on the choice of the codopants cocktail (Aluminum, Phosphorus) used to incorporate the rare-earth ions in the glass. More recently [17], we characterized the spectral dependence of the RIA for the same set of RE-doped fibers during and after exposure to high energy protons (105 MeV) or gamma-rays. These experiments also give new insights concerning the relative role of the RE-ions and of the glass matrix in the radiation-induced degradation. In this paper, we complete our previous work by studying the radiation-induced changes in the visible part of the spectrum for these five optical fibers. To do this, we used an ultraviolet (UV) laser operating at 5 eV to irradiate the optical fibers as we previously showed that this type of exposure can be less constraining and very useful to understand the effect of ionizing particles or photons [18].

## 2. EXPERIMENTAL PROCEDURE

### A. Tested optical fibers

We tested different RE-doped optical fibers, also called active optical fibers that can be used as part of amplifiers or other silica-based devices. In our work, we focused our study on silica-based glasses doped with Erbium (Er), Ytterbium (Yb) or Erbium/Ytterbium (Er/Yb) ions, with a particular emphasis for this paper on Yb and Yb/Er devices. The particular spectroscopic properties of these active ions allow designing amplifiers or laser sources in the third Telecom windows. Depending of the ions incorporated, the different fibers will be used at different wavelengths. As an example, if the two ions present strong absorption bands around 930-980 nm, the pumping at these wavelengths leads to emission at different wavelengths around 1 to 1.1 µm for Yb-doped samples and around 1.5 to 1.6 µm for Er and Er/Yb-doped optical fibers. As a consequence, the estimation of the fiber vulnerability is mainly made through online measurement of the radiation-induced attenuation (RIA) in the infrared range (900-1700 nm). However, to obtain a clear identification of the point defects involved in this RIA, it becomes also crucial to be able to measure this RIA at lower wavelength in the visible and if possible in the UV range. This kind of measurement is very difficult to perform especially for single-mode fibers, as our five samples, and this difficulty can be bypassed with the particular setup presented in this paper.

Previous studies showed that the incorporation of the RE-ions and the mechanisms of energy transfer between their energy levels depend on the nature of the host matrix. In addition to the dopants used for passive optical fibers like Germanium or Fluor, this kind of fibers is often doped with high levels of phosphorus and/ or aluminum. These two elements influence the RE-emitting centers optical properties and present some advantages like an improvement of the energy transfer efficiency mechanisms between $Yb^{3+}$ and $Er^{3+}$ ions, limitation of the clustering effects,…The main characteristics of the optical fiber samples tested in this work are presented in the following table:

| | [Yb] wt.% | [Er] wt.% | [Al] wt.% | [P] wt.% |
|---|---|---|---|---|
| F1 | 4.6 | none | none | 11.9 |
| F2 | 1.2 | none | 1.9 | none |
| F3 | 4.2 | none | 2.6 | 11.1 |
| F4 | 2.8 | 0.18 | none | 12.8 |
| F5 | 2.1 | 0.13 | 0.6 | 12.1 |

The three first fibers (F1-F3) are erbium-free; they are doped with ytterbium ($Yb^{3+}$) as luminescent ions and were chosen for their co-dopants composition reasons. F1 and F3 samples are both P co-doped with a similar amount and their comparison can highlight the effect of Al incorporation. F2 fiber is Al-doped (with no P) and it is used in this work in order to check the effect of this element alone, even if its corresponding Yb concentration is nearly four times smaller than the ones included in F1 and F3 samples. The F4 and F5 fibers are both Er-Yb co-doped, they have a similar amount of phosphorus and they are totally differentiated through the aluminum dopants.
Another important point is that these fibers have a double-cladd structure to ensure an efficient coupling of the pumping light from diodes into their RE-doped cores. This double-cladd is the same for the five samples and consists of pure-silica glass.

**Test procedures**

To understand the mechanisms at the origin of the RE-doped fibers degradation under irradiation, we performed different experiments which can be presented and assembled in two main parts:

1. **Online measurements** – This kind of experiment is essential when we want to quantify and follow, in real time, the evolution and modification of the optical properties of the material under irradiation in a certain spectral domain. Different experimental setups can be used to characterize the RIA during and after the irradiation. The radiation-induced losses can be measured with a passive setup configuration, i-e. without pumping and emission of the rare-earth ions. These measurements are done by using a white light source (WLS) for the probe signal and a spectrometer-detector for the analyses. Measurements are possible from the visible part of the spectrum to the near-IR (600 to 1700 nm for our tests). On the other hand, it is possible to measure the induced losses of a doped fiber in an active configuration i-e. by pumping of the RE ions with a laser source emitting in a spectral region of high absorbance and simultaneous measurements of the changes in their emission during the radiation exposure. However, the evaluation of the fiber response in the near UV spectral range is not easy to perform. The main difficulties are linked to: i) an intense UV light source with a well defined spectral properties, ii) this probe signal should be injected in the fiber core, iii) the fiber length should be long enough to allow the use of a cut-back technique, iv) even if these three previous points are gathered, it is not possible to quantify and separate the specific contributions generated by this intense probe UV signal from the part due to other kind of irradiations. To overcome these difficulties, we developed a specific technique [19] based on a transverse UV laser irradiation, at 244 nm, of the fiber sample which generate an intrinsic and guided emitted signal. This photoluminescence is ascribed to optically active centers located in the fiber core region and its intensity is sufficient enough for spectroscopic measurements. More details are given in the UV exposure experiments section.

2. **Post-mortem techniques –** These techniques are based on the analysis of the fiber samples before and after the irradiation and can give additional information concerning the permanent radiation-induced changes. Some "classical" luminescence measurements are usually performed in order to check the optical fiber response including both the RE ions and the active emitting centers generated by the irradiations. However, this method gives an integrated and non-local response of the waveguide. A powerful and adapted technique, based on a confocal microscopy of luminescence (CML) overcomes this problem and a short optical fiber length is needed for this measurement. In addition, the visited or checked region is limited to few microns square, so it is easier to distinguish and separate both the fiber core and the cladding zone. The principle of this technique consists in focusing a laser probe source (cw UV laser emitting at 325 nm in this work) through a microscope objective and

caring out a special filtering of the signal emitted by the illuminated volume, by using a diaphragm of small diameter placed in the conjugated plane where the magnified image of the sample is formed by the objective (X40). Luminescence spectra can be recorded from 340 nm up to 1100 nm with a spatial resolution of about 6-7 microns.

**Radiations facilities**

We used different radiation facilities to reproduce the environment associated with space missions. We have exposed our samples to high energy proton exposure at the TRIUMF facility, Vancouver [20]. Gamma-rays tests with $^{60}Co$ source can also be used to evaluate the vulnerability of a given fiber as low energy 10KeV X-rays provided by ARACOR machines. Furthermore, we previously showed the interest of ultraviolet (UV) exposures with 5eV photons to evaluate the fiber sensitivity to higher energy photons or particles.

## 3. EXPERIMENTAL RESULTS

In this section, we give some examples of our online experiments devoted on the estimation of the tested fiber vulnerability to space environment. We mainly focused the paper on the results obtained with UV exposures and own setup completing the previous experiments

### 1. Estimation of the different fiber radiation sensitivities

We estimate at the TRIUMF facility in Vancouver the degradation induced by 105 MeV and 50 MeV protons on the five different optical fibers with the passive and active configuration. We illustrate in Fig.1 the results obtained for one the tested optical fibers (fiber F2) during the exposure to 50 MeV protons at dose levels comparable to those encountered during the lifetime of a space mission. The induced losses have been measured in the whole range of wavelengths from 900 to 1700nm but only RIA growth and decay kinetics at 1 and 1.1µm are given in Fig. 1 as a function of the particle fluence.

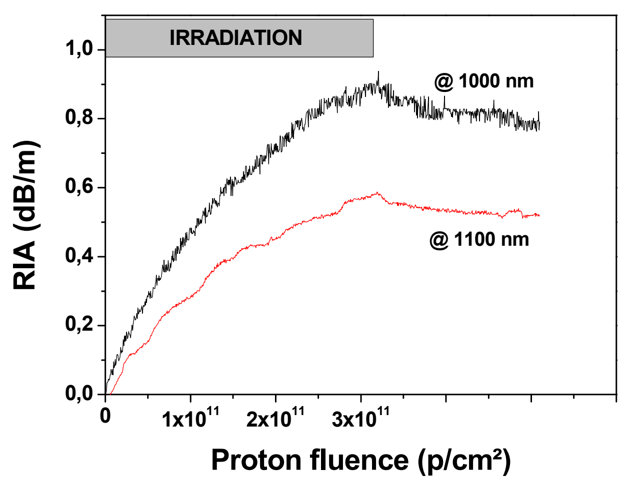


Fig. 1: RIA evolution in F2 fiber during a proton irradiation (at 50 MeV).

All the tested fibers exhibit an important increase of their linear attenuation during the exposure to protons at both energies or to gamma-rays and limited recovery of induced losses after the end of the exposure. However, the amplitudes and kinetics of these changes differ depending on the glass composition. We compare, in the figure 2, the spectral dependence of the RIA for the three Yb-doped fibers without Er at a fluence of 50 MeV protons corresponding to a dose of 25 krad(Si).

Fiber F3 presents lowest losses compared to the two other Yb-doped fibers (F1 and F2) in the IR part of the spectrum. The analysis of the spectral dependence of the induced losses reveals that the losses in fiber F1 are mainly related to an absorption band centered around 1600 nm, previously associated with the phosphorus-related P1 center.

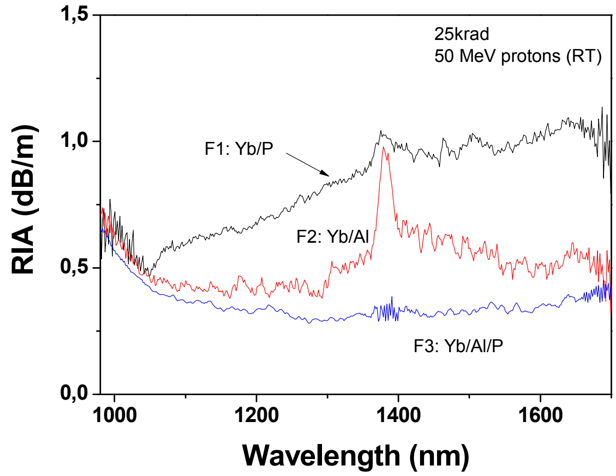


Fig. 2. Spectral dependence of the RIA for the Yb-doped fibers (F1-F3) during an exposure to protons irradiation (50 MeV) at a dose of 25 krad.

The additional codoping of the P/Yb doped glass with Al also reduces the contribution of this defect to the RIA for the Er/Yb –doped fiber F5 compared to the fiber F4 without Al. The comparison of the fibers with and without Er (F1 & F4 and F3&F5) does not reveal a strong influence of the Er-doping except around the absorption bands of the RE ions (around 980 and 1550nm).

## 2. UV exposure experiments

Fig.3 show the experimental set-up used for these kinds of measurements. The UV exposure is performed along a short fiber length, typically 20-30 cm. This irradiated part of the RE-doped samples is chemically stripped. The transverse irradiation is conducted with a cw UV laser operating at 244 nm with an output power of about 95 mW. For the spectroscopic measurements, a mini-spectrometer is connected at each end of the fiber. These apparatus can be used in the 240-1000 nm spectral range and their time response can be fixed to few ms. The study of the transverse UV laser irradiation influence is then performed while the fiber sample is moving along its longitudinal axis. Therefore, the fiber is fixed to a tight tread which can be pulled by a continuous motor at a constant speed. During the displacement, the sample passes through a fiber guide which leads to a homogeneous irradiation along the fiber axis and to avoid any misalignment of the fiber along the UV irradiation beam. Under these conditions, the detection system 2 remains constant whereas the detection 1 exhibits the evolution of the absorption spectra as the UV-induced-photoluminescence crosses the irradiated part of the fiber. In the near-UV spectral domain, the irradiation induced attenuation is so high that short lengths are needed to perform the complete measure.

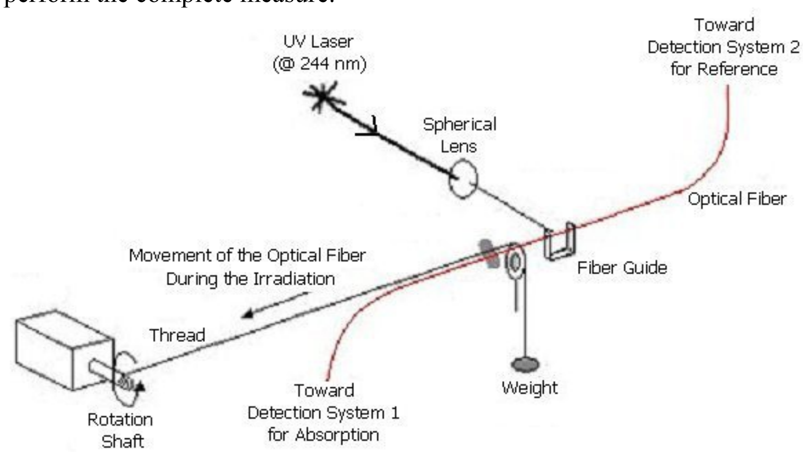


Fig. 3. Scheme of the UV online irradiation experimental set-up

As pointed out in the previous section, the transverse UV laser irradiation, at 244 nm, leads to a generation of a guided photoluminescence signal which can be used as an interesting probe signal to check the waveguide in a quite large spectral domain starting with wavelengths lower than 300 nm.

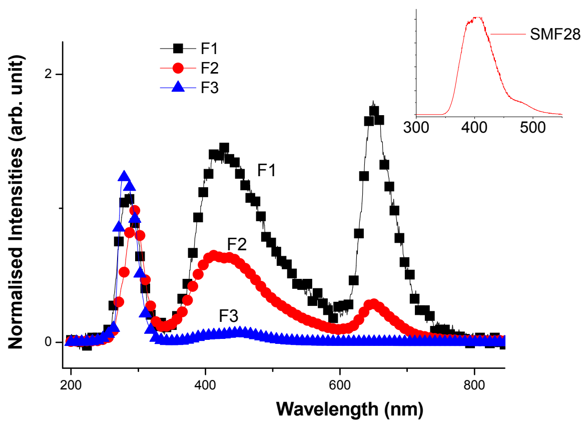


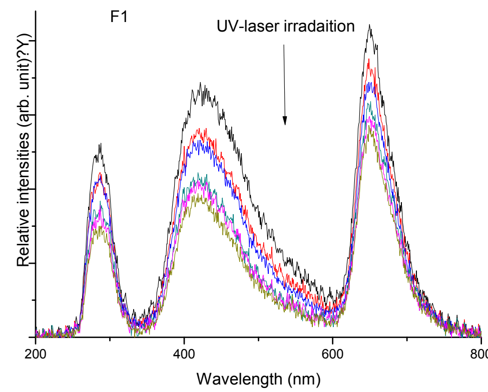


Fig. 4. Normalized photoluminescence spectra recorded under a transverse UV laser irradiation at 244 nm on sample F1 (■), F2 (●) and F3 (▲). In the inset: we report the response of a well known SMF28 fiber which highlights the main differences due to the fiber dopants with no signal around 650 nm.

Fig. 5. Online evolution of the photoluminescence spectra of the F1 fiber during the UV laser exposures.

The main photoluminescence bands are located around 290 nm, 400-430 nm and 650 nm. A large part of the two first ones are usually attributed to oxygen deficient centres –such as Lone pair centres whose singlet – singlet transition is located around 290 nm whereas the triplet- singlet transition is in the 400 nm wavelength range. The third emission band overlaps the well known Non Bridging Oxygen Hole Centres –NBOHC- whose optical signature is in this spectral range. These two kinds of defects can be generated during the fibre elaboration-drawing phases and their concentrations depend on dopants included initially in the fiber composition.

The three fibers exhibit different optical responses. Despite their specific composition, a certain similitude can be observed in the F1 and F2 fibers. It seems that the incorporation of Al or P (one at a time) favorites the formation of structures with non coupled electron. Whereas, the combination of these two co-dopants –together- has a drastic effect as no signal is detected at around 650 nm. This positive influence also affects the P-defects concentration, which play a significant role in the infra-red domain where the RE ions are active. We observed similar properties and evidenced similar behavior type when these fibers were submitted to energetic protons or X-rays irradiations. In that case, the main investigations were performed in the IR domain whereas these UV measurements focus in the near UV – visible spectral range. In the inset of figure 4, we report, for a guide eye or as a reminder, the signal detected in SMF28 "classical" fiber. The fiber composition (nature and concentration) is therefore one of the important part to study.

As the fibre is moving during the UV – irradiation, Figure 3, it is possible to follow the evolution of UV irradiation influence on the emitted signal attenuation (Fig.5). We therefore extract the absorption coefficients, at a given wavelength, which are estimated to be within $10^{-2}$ $mm^{-1}$ at 425 nm and 5 $10^{-3}$ $mm^{-1}$ at around 290 nm in F1 sample. The corresponding values in the F3 sample are: 2 $10^{-2}$ $mm^{-1}$at 280 nm and 7 $10^{-3}$ mm-1 at 410 nm (Fig 6).

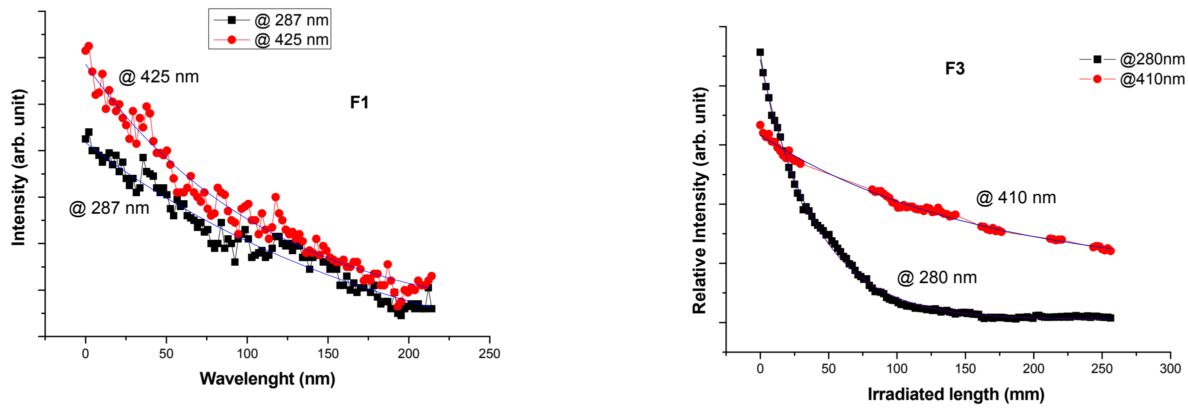


Fig. 6: Evolution of the UV-induced emitted signals as a function of the irradiated fiber length in the F1 and F3 samples.

The incorporation of $Er^{3+}$ ions effect is thus easy to observe through the analyses of F1 and F4 samples. Our results, Fig.7, clearly show that the erbium ions do not modify the optical response of the fiber. However, the emission band located in the blue part of the UV-laser induced emission exhibits a structured profile as this spectral domain is in phase with the erbium ions absorption. Otherwise, the near-UV-visible studied spectral domain is not affected by the addition of the erbium ions.
The comparison between F4 and F5 reinforces the fact that the P-centres formation and thus their influence on the fibre performances-degradation are countered by the addition of Al elements.

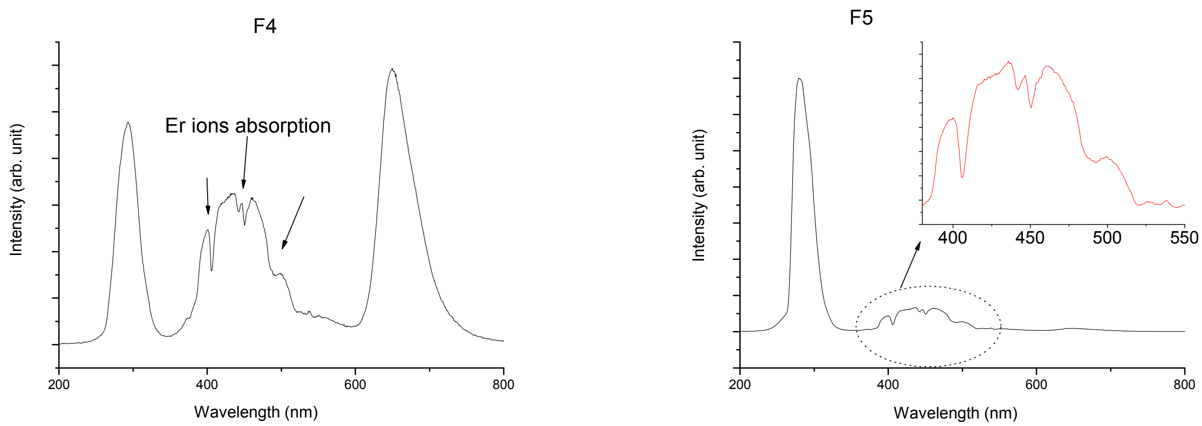


Fig. 7: Photoluminescence spectra recorded under a transverse UV laser irradiation at 244 nm on F4 (left) and F5 (right) samples. In the inset: we report a zoom of 380-550nm region where the $Er^{3+}$ ions absorption signatures are clearly identified

## 4. CONCLUSION

This work highlights the relative influence of the Al and P co-doping on the radiation response of rare-earth doped optical fibers. We completer online measurements of the radiation-induced attenuation with additional measurements of spectroscopic changes induced by 5 eV ultraviolet exposure. The RIA observed in samples doped with only one of these

elements is neutralised par the presence of the second one. The possible routes and elementary mechanisms for the defects formations are really reduced when these two elements coexist together.
In another plan, the UV-laser irradiation used in this work permit us to quantify the absorption coefficients of these fibre types and they are estimated to be within: 0.005 $mm^{-1}$ - 0.15 $mm^{-1}$. One practical advantage of this UV-irradiation technique resides in the quite short fibre lengths which are needed to perform the measurements.

# 5. REFERENCES


[1] D.L. Griscom, "The natures of point defects in amorphous silicon dioxide", in G. Pacchioni, L. Skuja and D.L. Griscom (Eds), Defects in SiO2 and related Dielectrics, Kluwer, 117-160 (2000).

[2] R. A. B Devine. and J. M. Francou, "Extrinsic- and intrinsic defect creation in amorphous silica", Phys. Rev. B, vol. 41, 12882-12887 (1990).

[3] D. L.Griscom, "Optical properties and structures of defects in silica glass", J. of Ceramic Soc. of Japan, vol. 99, 899-916 (1991).

[4] E. J. Friebele, "Photonics in the space environment", IEEE Nuclear and Space Radiation Effects Conference, San Diego, Short Course, pp. III-1 - III-25, (1991).

[5] F. Berghmans, et al., "An introduction to radiation effects on optical components and fiber optic sensors", in "Optical Waveguide Sensing and Imaging", NATO Science for Peace and Security Series, Springer, (2008).

[6] S. Girard, "Analyse de la réponse des fibres optiques soumises à divers environnements radiatifs," PhD Thesis, Université de Saint-Etienne, France, (2003).

[7] M. Leone, S. Agnello, R. Boscaino, M. Cannas, F.M. Gelardi, "Optical absorption, luminescence and ESR spectral properties of point defects in silica", in H.S. Nalwa (Ed), Silicon-based Materials and Devices, vol.2, "Properties and Devices", Academic Press, 1-50, (2001).

[8] L. Skuja, "Optical properties of point defects in silica", in G. Pacchioni, L. Skuja and D.L. Griscom (Eds), Defects in SiO2 and related Dielectrics, Kluwer, pp. 73-116, (2000).

[9] H. Henschel, O. Köhn, H.U. Schmidt, J. Kirchhof, S. Unger, "Radiation induced loss of rare earth doped silica fibers", IEEE Trans. Nuc. Sci., 45, 3, 1552–1557, (1998).

[10] M.W. Wright, and G.C. Valley, "Yb-Doped Fiber Amplifier for Deep-Space Optical Communications", IEEE Journal of Lightwave Technology, 23, 3, 1369-1374, (2005).

[11] E. J. Friebele, et al., "Correlation of single mode fiber fabrication factors and radiation response", Naval Research Laboratory, Washington, D.C NRL/MR/6505-92-6939, February 28th, (1992).

[12] S. Girard, et al., "Transient radiation responses of silica based optical fibers: influence of Modified Chemical Vapor Deposition process parameters", Journal of Applied Physics, 99, 023104, (2006).

[13] B. Brichard and A. F. Fernandez, Short Course RADECS 2005 – New Challenges for radiation tolerance assessment from deep space environments to fusion reactor environments, chapter Radiation Effects in silica glass optical fibres, 95-138., (2005).

[14] S. Girard, J. Keurinck, Y. Ouerdane, J-P. Meunier, and A. Boukenter, "g -rays and Pulsed X-ray Radiation Responses of Germanosilicate Single-Mode Optical Fibers: Influence of Cladding Codopant", IEEE Journal of Lightwave Technology 22, 1915-1922 (2004).

[15] B. Tortech, S. Girard, E. Régnier, Y. Ouerdane, A. Boukenter, J-P. Meunier, M. Van Uffelen, A. Gusarov, F. Berghmans, H. Thienpont, "Core versus cladding effects of proton irradiation on erbium-doped optical fiber: micro-luminescence study" IEEE Trans. Nucl. Sc. 55, 4, (2008).

[16] B. Tortech, Y. Ouerdane, S. Girard, J.P. Meunier, A. Boukenter, T. Robin, B. Cadier, P. Crochet, "Radiation effects on Yb- and Er/Yb-doped optical fibers: a micro-luminescence study" To be published in JNCS (accepted).

[17] S. Girard, Y. Ouerdane, B. Tortech, C. Marcandella, T. Robin, B. Cadier, J. Baggio, P. Paillet, V. Ferlet-Cavrois, A. Boukenter, J-P. Meunier, J.R. Schwank, M.R. Shaneyfelt, P.E. Dodd, E.W. Blackmore, "Radiation Effects on Yb- and Yb/Er-doped Double-Clad Optical Fibers", Nuclear and Space Radiation Effects Conference, Quebec, (Canada) July 20 – 24 (2009).

[18] S. Girard, B. Vincent, J-P. Meunier, Y. Ouerdane, A. Boukenter, A. Boudrioua, "spatial distribution of the red luminescence in pristine, g -rays and UV-irradiated optical fibers", Appl. Phys. Lett. 84, 4215-4217 (2004).

[19] B. Tortech, Y. Ouerdane, A. Boukenter, J-P. Meunier, S. Girard, M. Van Uffelen, E. Régnier, F. Berghmans and H. Thienpont, "Transverse UV laser irradiation-induced defects and absorption in a single mode Erbium-doped optical fiber", To be published in Opt. Mat. (accepted).
[20] E. Blackmore, "Operation of the TRIUMF (20–500 MeV), proton irradiation facility" IEEE Radiation Effects Data Workshop Record, Reno, Nevada, pp.1-5, (2000).